WindSat Applications for Weather Forecasters and Data Assimilation

Thomas Lee, James Goerss, Jeffrey Hawkins, Joseph Turk
Naval Research Laboratory
7 Grace Hopper Avenue
Monterey CA

Zorana Jelenak, Paul Chang
NOAA-NESDIS

***Abstract*-This paper examines WindSat wind retrievals from two perspectives. The first is a statistical analysis, comparing both WindSat and QuikSCAT to model output. The second is an analysis geared toward weather forecasters based on individual case studies.**

I. COMPARISON TO NAVDAS/NOGAPS

We compared WindSat and QuikSCAT observations against the NRL Monterey Atmospheric Variational Data Assimilation System (NAVDAS) 10m wind analyses for October 2003-February 2004. NAVDAS [1] routinely initializes the Navy Operational Global Atmospheric Prediction System (NOGAPS). The WindSat data came from a data set, intended for research and development only, put out by the Physical Oceanography data distribution center at the Jet Propulsion Laboratory in Pasadena California. We only examined observations for which the wind speed was less than or equal to 20 m/s and all flags but the Wind Speed Flag were zero. The QuikSCAT data [2] are the operational retrievals from the U.S. Navy's Fleet Numerical Meteorology and Oceanography Center (FNMOC) in Monterey California. For QuikSCAT we only examined observations for which the wind speed was less than or equal to 20 m/s and both the Rain Flag and Edge of Swath Flag were zero. Statistics were computed for the differences between the observed and analysis wind directions and wind speeds for WindSat and QuikSCAT and were stratified by NAVDAS analysis wind speed. We computed global statistics for the entire 5-month period as well as for October, December, and February.

The operational NOGAPS/NAVDAS 10m wind analyses for October 2003-February 2004, available four times a day (00, 06, 12, and 18 UTC), were used as the baseline for this comparison of WindSat and QuikSCAT vector wind observations. The 10m wind analysis fields come from half-degree global grids and are at approximate 55 km resolution, the nominal resolution of the NOGAPS T239 spectral forecast model. None of the analyses made during this period used any scatterometer winds or passive microwave wind speeds.

For each analysis time, the WindSat and QuikSCAT observations within a two-hour window centered on the analysis time were compared with the analysis wind at the observation location. Only WindSat and QuikSCAT observations that had two or more ambiguities were considered. For both sensors, the observation chosen was the one whose wind direction was closest to and within 90 degrees of the analysis wind direction at the observation location.

We examined global statistics for the five-month period for WindSat and QuikSCAT observations with wind speeds less than or equal to 20 m/s. The total number of observations for WindSat and QuikSCAT were just over 41 million and just over 29 million, respectively. The distribution of the observations with respect to the global analysis is quite similar for each sensor. We found that 61.3% of the WindSat observations and 60.6% of the QuikSCAT observations occurred when the analysis wind speed was less than or equal to 7.5 m/s. The respective percentages when the analysis wind speed was less than or equal to 10 m/s were 83.3% and 81.5%. The wind speed and direction standard deviations for the two sensors with respect to the NOGAPS/NAVDAS analyses are displayed in Fig. 1. The WindSat standard deviations are smaller (greater) than those for QuikSCAT for wind speeds less (greater) than 10 m/s. As expected, the wind direction standard deviations for QuikSCAT are less than those for WindSat for all wind speed ranges but by only 2-3 degrees for analysis wind speeds greater than 7.5 m/s. For analysis wind speeds greater than 7.5 m/s, the wind direction standard deviations for the WindSat wind vectors are less than 20 degrees (39% of the observations). The wind direction standard deviations for the QuikSCAT wind vectors are less than 20 degrees for analysis wind speeds greater than 5 m/s (71 % of the observations).

Report Documentation Page

Form Approved
OMB No. 0704-0188

1. REPORT DATE **25 JUL 2005**	2. REPORT TYPE **N/A**	3. DATES COVERED **-**

4. TITLE AND SUBTITLE **WindSat Applications for Weather Forecasters and Data Assimilation**	5a. CONTRACT NUMBER 5b. GRANT NUMBER 5c. PROGRAM ELEMENT NUMBER
6. AUTHOR(S)	5d. PROJECT NUMBER 5e. TASK NUMBER 5f. WORK UNIT NUMBER
7. PERFORMING ORGANIZATION NAME(S) AND ADDRESS(ES) **Naval Research Laboratory 7 Grace Hopper Avenue Monterey CA**	8. PERFORMING ORGANIZATION REPORT NUMBER
9. SPONSORING/MONITORING AGENCY NAME(S) AND ADDRESS(ES)	10. SPONSOR/MONITOR'S ACRONYM(S) 11. SPONSOR/MONITOR'S REPORT NUMBER(S)

12. DISTRIBUTION/AVAILABILITY STATEMENT
Approved for public release, distribution unlimited

13. SUPPLEMENTARY NOTES
See also ADM001850, 2005 IEEE International Geoscience and Remote Sensing Symposium Proceedings (25th) (IGARSS 2005) Held in Seoul, Korea on 25-29 July 2005. , The original document contains color images.

14. ABSTRACT

15. SUBJECT TERMS

16. SECURITY CLASSIFICATION OF:			17. LIMITATION OF ABSTRACT	18. NUMBER OF PAGES	19a. NAME OF RESPONSIBLE PERSON
a. REPORT **unclassified**	b. ABSTRACT **unclassified**	c. THIS PAGE **unclassified**	**UU**	**4**	

Standard Form 298 (Rev. 8-98)
Prescribed by ANSI Std Z39-18

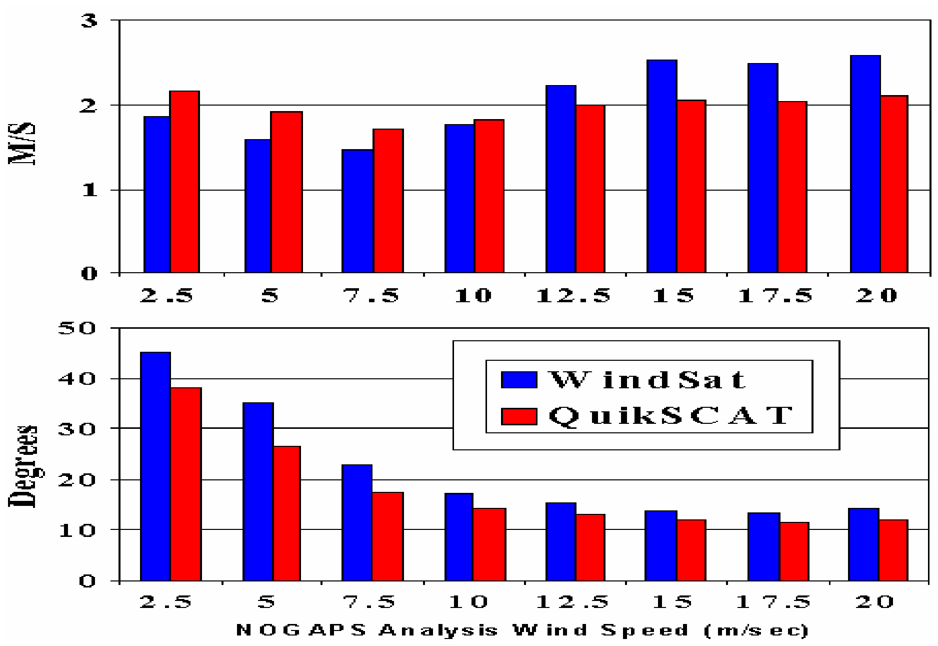

Fig. 1 WindSat and QuikSCAT standard deviations, both with respect to NAVDAS/NOGAPS. Top: Wind speed. Bottom: Wind direction.

II. CASE STUDIES

A. Rain Contamination in a Frontal System

The version of WindSat retrievals shown in this section is still relatively immature (Version 0; [3]), and includes wind vectors, total precipitable water (TPW), total cloud water (TCW), and sea surface temperature. The first three are shown in Fig. 2A-C, with a comparison to QuikSCAT ([2]; 99 min earlier in Fig. 2D). The gradient in TPW identifies the cold front [4] on the poleward side of a moist plume marking the frontal zone (Fig. 2A). Generally, TCW values higher than 0.2 kg/m2 (darker reds shades on Fig. 2B) indicate probable precipitation and significant wind vector contamination. However, we do not flag contamination on Fig. 2C in order to examine vector behavior in cloudy, rainy regions. Contaminated QuikSCAT retrievals, on the other hand, are flagged in black, e.g., in the frontal zone.

Fortunately, over most of the WindSat pass, the vectors do not occur in regions of high CLW. Within the frontal zone where the retrievals are degraded, wind speeds exceed 50 knots (25 m/s) along the front. These speeds are much higher than nearby retrievals and almost certainly biased high. For example, corresponding QuikSCAT retrievals in the frontal zone are only about 30 knots. However, the directions of the 50 knot+ retrievals do not appear entirely unreasonable, marking a shift from north-northwest north of the front to southwest to the south. However, the directions do not agree with QuikSCAT, a sensor with less sensitivity to clouds and precipitation, at about the same time, that shows a less sharp shift in wind direction along the front (Fig. 2D).

We have noticed this trend, of high-bias wind speeds but somewhat reasonable directions, in a variety of frontal systems studied with the Version 0 retrievals. This is consistent with the derivation of the wind vectors from the Stokes Vector. The derivation of wind speed comes from the first and second Stokes Vectors. These parameters are very sensitive to atmospheric influence, particularly cloud cover as in Fig. 2B in the frontal zone. Clouds and rain impart a significant high bias to retrieved wind speed values, a similar problem observed in retrievals from the Special Sensor Microwave Imager (SSM/I), a predecessor to WindSat [5]. However, the retrieval of wind direction is based on the third and fourth Stokes Parameters, which though still sensitive to the atmosphere, are less so than the first and second.

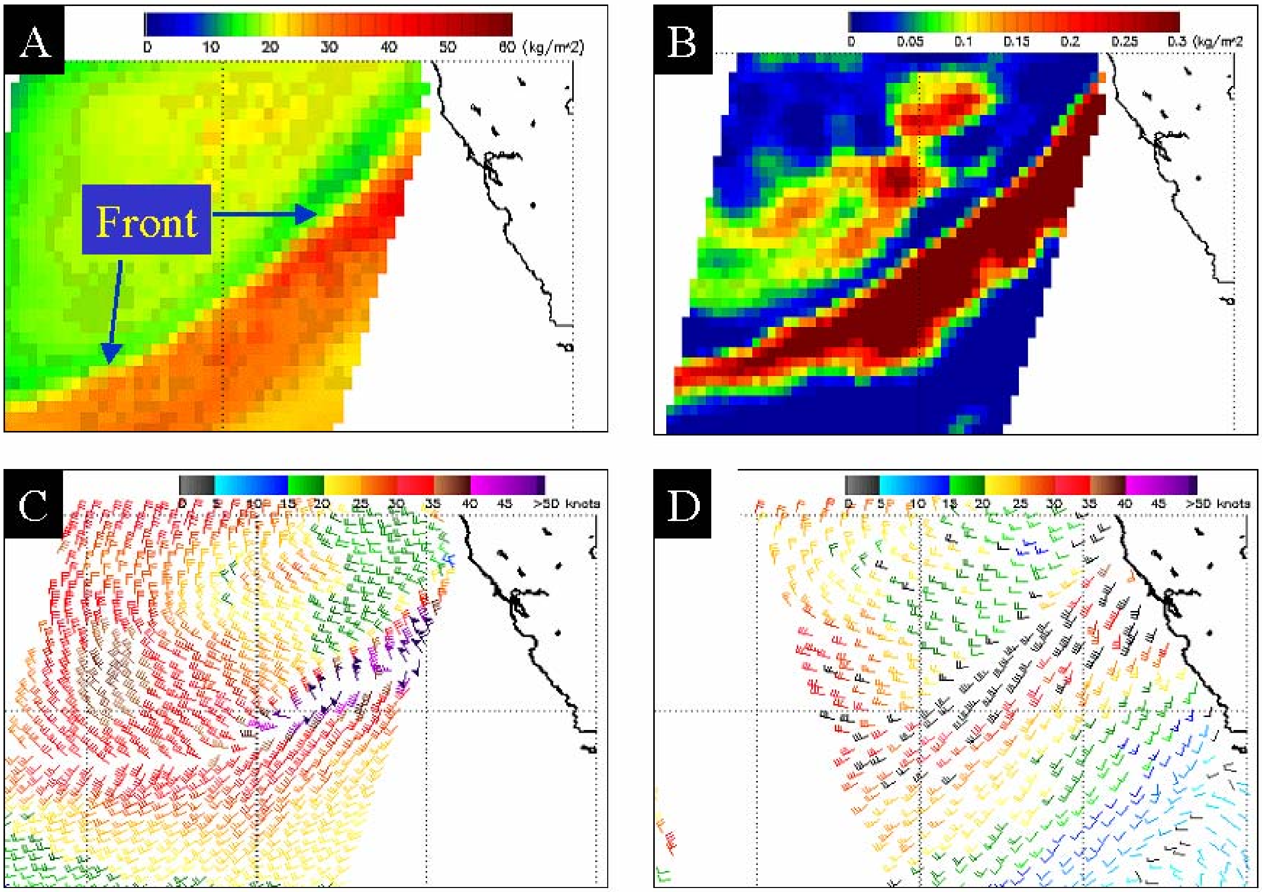

Fig. 2 Pacific Frontal System, 29 December 2003. A) Windsat TPW 1511 UTC; B) Windsat TCW 1511 UTC; C) WindSat wind vectors 1511 UTC; D) QuikSCAT wind vectors 1342 UTC.

B. Topographically-induced Phenomena

Some of the most operationally useful features in WindSat vector plots are due to topographic effects relatively near shore. No retrievals are possible closer than about 25-50 km from shore. Downwind (northeast) of Socorro Island green vectors represent reduced wind speeds due to the island sheltering effect (Fig. 3A). Fig. 3B shows the Tehuanteper gap wind south of Mexico. Notice the strongest winds are nearest to the coast near the exit region of the gap. Fig. 3C shows a gap wind between Sir Lanka and India, and Fig. 3D shows a gap wind downwind of Japan. Figs. 3B-D document that gap winds extend great distances over the ocean regions. Cloud and rain contamination are relatively uncommon in these wind systems due to their continental sources.

WindSat represents a major advance in the ability to study such systems. Previous passive microwave products showed the wind speeds associated with the gap winds, but wind directions were lacking. Directions missing from SSM/I retrievals could only be supplied from corresponding model output [6]. Despite missing directions, SSM/I winds helped validate mesoscale model forecasts of topographically-induced winds [7].

When the National Polar Orbiting Environmental Satellite System (NPOESS) Conical Microwave Imager Sounder (CMIS) comes online at the end of this decade the ability to observe gap winds will increase substantially. When the NPOESS constellation is fully manifested, three satellites will orbit. CMIS coverage, 1700 km wide, will be substantially greater than Windsat. Due to an extremely fast worldwide data relay system, products will arrive in front of forecasters in about 30 min after overpass. With retrieval of both speed and direction, CMIS should lead to improvements in mesoscale forecast validation. Data delivery will be even faster at sites capable of direct reception of NPOESS raw data as the satellite passes overhead. Such sites include aircraft carriers of the United States Navy.

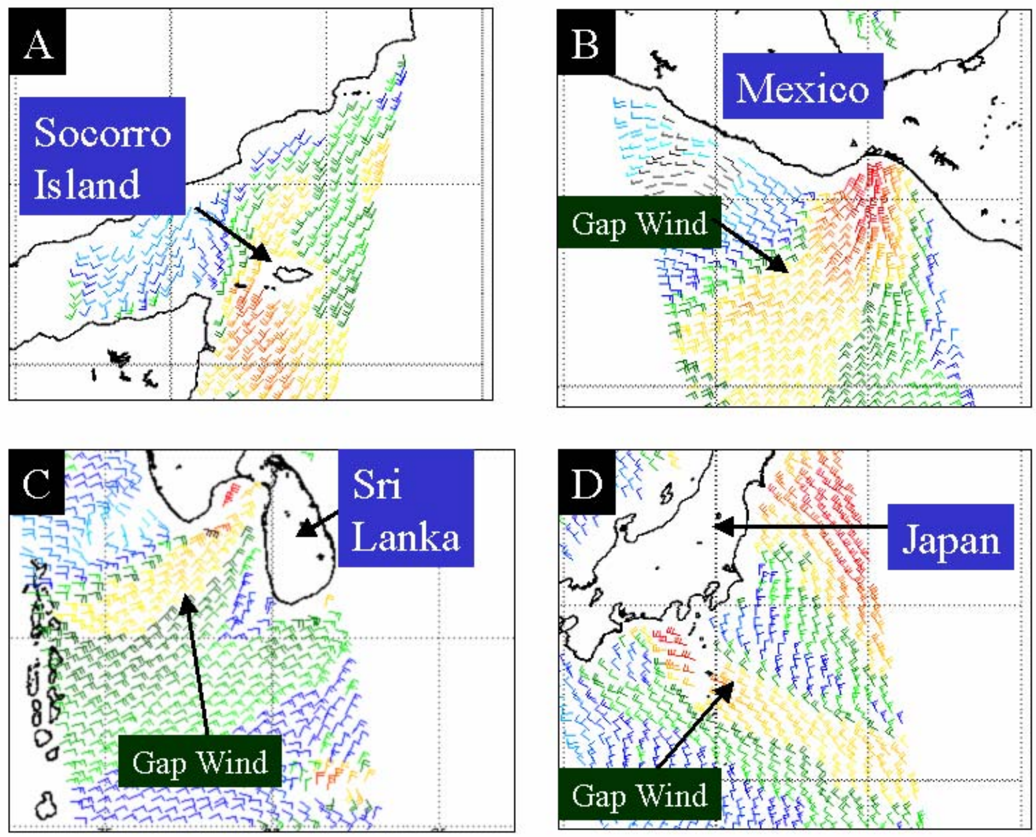

Fig. 3 Topographically-induced wind regimes. A: Low wind speeds downwind of Socorro Island, Arabian Sea, 9 September 2003; B. Tehuantepecer gap wind, 19 December 2003; C. Gap wind between Sri Lanka and India, 10 January 2004; D. Japanese gap wind, 19 December 2003. Wind color convention from Fig. 2C.

ACKNOWLEDGMENTS

The support of the research sponsor, the National Polar-orbiting Operational Environmental Satellite System's (NPOESS) Integrated Program Office (IPO) located in Silver Spring, MD, is gratefully acknowledged.

REFERENCES

[1] R. Daley, and E. Barker, "NAVDAS: Formulation and Diagnostics," *Mon. Wea. Rev.,* vol. 129, pp. 869-883, April 2001.

[2] J.M. Augenbaum, R.W. Luczak, and G. Legg, **"**Seawinds near-real-Time processing at NOAA/NESDIS: present status and future plans," *Proceedings American Meteorological Society (Interactive Information and Processing Systems),* Long Beach California, January 2003.

[3] Z. Jelenak, T. Mavor, L. Connor, N-Y. Wang, P.S. Chang and P. Gaiser, "Validation of ocean wind vector retrievals from WindSat polarimetric measurements," in *Proceedings of 4th International Asian-Pacific Environmental Remote Sensing Conference,* Honolulu HI., pp. 111-121, December 2005.

[4] K.B. Katsaros, B. Iftekhar, L.A. McMurdie, and G.W. Petty, "Identification of atmospheric fronts over the ocean with microwave measurements of water vapor and rain," *Wea. Forecasting*, vol. 4, pp. 449-460, September 1989.

[5] M.A. Goodberlet, C.T. Swift, and J.C. Wilkerson, "Ocean surface wind speed measurements of the Special Sensor Microwave/Imager (SSM/I)," *IEEE Trans. Geoscience Remote Sens.,* vol. 28, pp. 823-828, September 1990.

[6] Thomas F. Lee and J.S Boyle, "A synoptic comparison of SSM/I winds with output from an operational forecast system," *Wea. Forecasting*, vol. 6, pp. 404-410, September 1991.

[7] J.E. Nachamkin, "Mesoscale verification using meteorological composites," *Mon. Wea. Rev.,* vol. 132, pp. 941-955, April 2004.